Supporting Information

A lanthanide tag for a complementary set of pseudocontact shifts

Lydia Topping,[a] Adarshi P. Welegedara,[b] Martyna Judd,[c] Elwy H. Abdelkader,[b] Nicholas Cox,[c] Gottfried Otting[b] and Stephen J. Butler[a]*

[a] Department of Chemistry, Loughborough University, Epinal Way, Loughborough, LE11 3TU, United Kingdom.

[b] ARC Centre of Excellence for Innovations in Peptide & Protein Science, Research School of Chemistry, Australian National University, Canberra, ACT 2601, Australia

[c] Research School of Chemistry, Australian National University, Canberra, ACT 2601, Australia

Synthesis and characterisation of ligand C14 and corresponding Ln(III) complexes

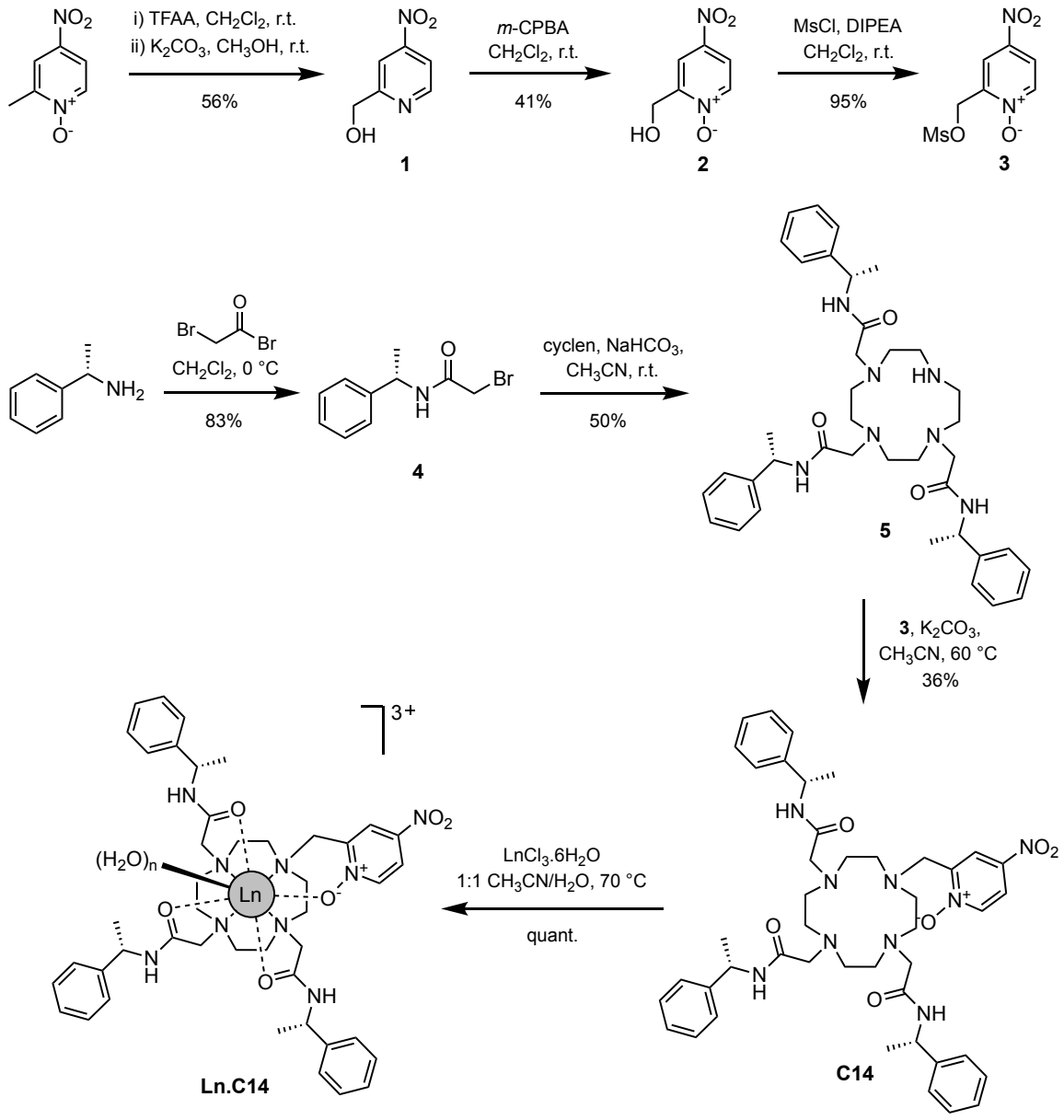

Scheme S1. Synthetic scheme for the lanthanide(III) tag **Ln.C14**

High Performance Liquid Chromatography

Preparative RP-HPLC was performed using a Waters 2489 UV/Visible detector performed at 254 nm, a Waters 1525 Binary HPLC pump controlled by the Waters Breeze 2 HPLC system software. Separation was achieved using a semi-preparative XBridge C18 (5 µm OBD 19 × 100 mm) column at a flow rate maintained at 17 mL/min. A solvent system composed of water (0.05% formic acid) / methanol (0.05% formic acid) was used over the stated linear gradient. Analytical RP-HPLC was performed using a XBridge C18 (5 µm 4.6 × 100 mm) column at a flow rate maintained at 2.0 mL/ min using the stated gradient and solvents.

The synthetic procedures for compounds **1**, **4** and **5** was followed according to our previous publication and are reproduced here.[1]

2-(Hydroxymethyl)-4-nitropyridine (1)

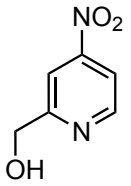

1

To a solution of commercially available 2-methyl-4-nitropyridine-1-oxide (1.00 g, 6.50 mmol) in CH_2Cl_2 (20 mL) was slowly added trifluoroacetic anhydride (1.90 mL, 13.0 mmol) in CH_2Cl_2 (3 mL) and the reaction mixture was stirred at room temperature for 72 hours. The solvent was removed under reduced pressure and the resulting yellow oil was dissolved in methanol (10 mL) and saturated K_2CO_3 solution (5 mL) and stirred at room temperature for 24 hours. The solvent was removed under reduced pressure and the white solid was partitioned between water (30 mL) and ethyl acetate (50 mL) and extracted with ethyl acetate (2 × 50 mL). The combined organic layers were dried over $MgSO_4$, filtered and the solvent was removed under reduced pressure. The alcohol **1** was obtained as a pale yellow solid (560 mg, 56%). No further purification was required. ^{1}H NMR (400 MHz, $CDCl_3$) δ 8.86 (d, J = 5.5 Hz, 1H), 8.09 (s, 1H), 7.94 (d, J = 5.5 Hz, 1H), 4.93 (s, 2H), O-H signal not observed. The NMR data are in agreement with those reported previously.[1]

2-(Hydroxymethyl)-4-nitropyridine 1-oxide (2)

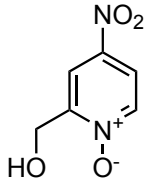

2

A solution of methyl alcohol **1** (2.00 g, 13.0 mmol) in CH_2Cl_2 (160 mL) was cooled to 0°C for 5 minutes. *m*-CPBA (2.47 g, 14.3 mmol) was added slowly, and the mixture was allowed to warm to room temperature and stirred for 22 hours. Saturated aqueous $NaHCO_3$ solution (80 mL) was added and the mixture was stirred for 10 minutes. The aqueous layer was extracted with CH_2Cl_2 (3 × 100 mL) and the combined organic layers were washed with brine (2 × 80 mL), dried over magnesium sulfate and concentrated under reduced pressure. The crude material was purified by column chromatography (silica gel; 0–10% MeOH in CH_2Cl_2) to give the desired N-oxide **2** (0.901 g, 41% yield) as a white solid. ^{1}H NMR (400MHz, CD_3CN) δ: 8.27 (d, J = 7.0 Hz, 1H), 8.25 (d, J = 3.3 Hz, 1H), 8.05 (dd, J= 7.0, 3.3 Hz, 1H), 4.65 (s, 2H). ^{13}C NMR (125 MHz, CD_3CN) δ: 154.3, 143.8, 141.1, 119.7, 118.7, 59.6. HRMS (ESI+) calculated for $[M+H]^+$, $[C_6H_7N_2O_4]^+$ *m/z* 171.0406, found 171.0401. R_f = 0.43 (CH_2Cl_2/MeOH 96:4).

(*S*)-2-Bromo-*N*-(1-phenylethyl)acetamide (4)

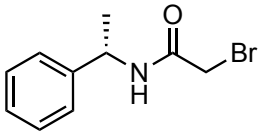

4

A solution of (*S*)-1-phenylethan-1-amine (6.38 mL, 49.5 mmol) in CH_2Cl_2 (25 mL) was added dropwise to a solution of bromoacetyl bromide (2.16 mL, 27.8 mmol) in CH_2Cl_2 (75 mL) at 0 °C under a nitrogen atmosphere. Following complete addition, the reaction was stirred for 2 hours and allowed to equilibrate to room temperature. The reaction mixture was washed with a 2M hydrochloric acid solution (50 mL) followed by brine (50 mL). The organic layer was dried with $MgSO_4$ and the solvent was removed under reduced pressure to give (*S*)-2-bromo-*N*-(1-phenylethyl)acetamide **4** (5.54 g, 83%) as a white solid. No further purification was required. ^{1}H NMR (500 MHz, $CDCl_3$) δ 7.40–7.25 (m, 5H), 5.08 (d, J = 7.0 Hz, 1H), 3.95–3.82 (dd, J = 22.9 Hz, J = 13.7 Hz, 2H), 1.52 (d, J = 7.0 Hz, 3H). ^{13}C NMR (125 MHz, $CDCl_3$) δ: 164.6, 142.4, 128.9, 128.6, 127.7, 126.2, 49.7, 29.4, 21.8.

IR (ν_{max}/cm^{-1}, neat): 3257, 3060, 2977, 1644, 1543, 1205. HRMS (ESI+): calculated for $[M+Na]^+$, $[C_{10}H_{12}NOBrNa]^+$ *m/z* 263.9994, found 263.9995. The NMR data are in agreement with those reported previously.[1]

2,2′,2″-(1,4,7,10-Tetraazacyclododecane-1,4,7-triyl)tris(*N*-((*S*)-1-phenylethyl)acetamide) (5)

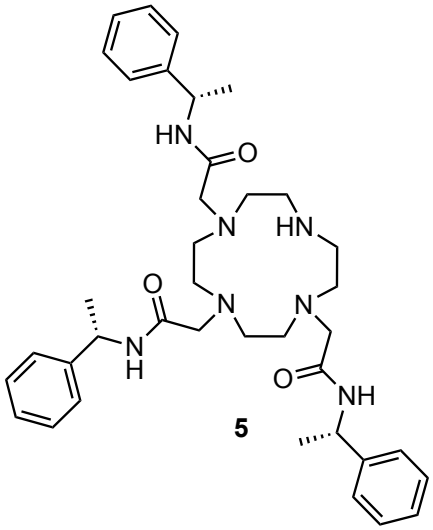

5

A solution of (*S*)-2-bromo-*N*-(1-phenylethyl)acetamide **4** (0.703 g, 2.90 mmol, 2.5 equiv.) in CH_3CN (10 mL) was added dropwise to a stirred mixture of cyclen (0.200 g, 1.16 mmol) and $NaHCO_3$ (0.243 g, 2.90 mmol) in CH_3CN (50 mL), under a nitrogen atmosphere at room temperature. The reaction mixture was stirred for a further 24 hours, then the solvent was removed under reduced pressure. The residue was dissolved in CH_3Cl (50 mL) and was transferred to a separating funnel. Water (150 mL) was added, and after vigorous shaking the pH was adjusted to 3. The organic layer was isolated and the aqueous phase was washed with CH_3Cl (2 × 50 mL). This procedure was repeated at pH 5, 6 and then 7 to isolate the desired product from over-alkylated byproduct. The organic layers containing the desired product (determined by LCMS analysis) were combined, dried over $MgSO_4$ and the solvent was removed under reduced pressure. The crude material was then purified by column chromatography (silica gel, CH_2Cl_2/NH_3 99.5/0.5, to $CH_2Cl_2/CH_3OH/NH_3$ 88/12/0.5, in 2% increments) to give compound **5** (0.723 g, 50%) as a pale yellow solid. ^{1}H NMR (400 MHz, $CDCl_3$) δ: 7.50–7.00 (m, 15H), 5.10–4.80 (m, 3H), 3.40–3.00 (m, 6H), 2.70–2.20 (m, 16H), 1.60–1.30 (m, 9H). ^{13}C NMR (100 MHz, $CDCl_3$) δ: 171.7, 171.2, 144.1, 143.9, 128.5, 127.2, 126.7, 126.5, 60.5, 56.9, 55.3, 54.8, 51.9, 50.0, 49.2, 46.5, 22.6, 21.7. IR(ν_{max}/cm^{-1}, neat): 3230, 3030, 2980, 1644, 1534, 1448. R_f (10% CH_3OH/CH_2Cl_2)

= 0.2. HRMS (ESI+): calculated for $[M+H]^+$, $[C_{38}H_{54}O_3N_7]^+$ *m/z* 656.4283, found 656.4277. The NMR data are in agreement with those reported previously.[1]

Ligand C14

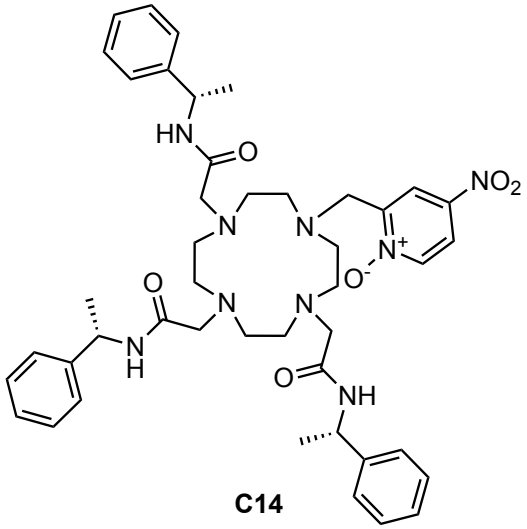

C14

Step 1: To a solution of N-oxide **2** (250 mg, 1.47 mmol) and DIPEA (510 µL, 2.90 mmol) in anhydrous CH_2Cl_2 (20 mL) was added methansulfonyl chloride (102 µL, 1.32 mmol). The solution was then stirred at room temperature for 20 hours. The reaction mixture was washed with brine (2 × 10 mL), dried over $MgSO_4$ and concentrated under reduced pressure to give the mesylate ester **3** (344 mg, 93%) as a colourless oil, which was used immediately in the next step.

Step 2: To a solution of macrocycle **5** (0.450 g, 0.690 mmol) in anhydrous CH_3CN (60 mL) was added potassium carbonate (0.270 g, 1.95 mmol) and the mixture was stirred for 5 minutes. The mesylate ester **3** (0.344 g, 1.39 mmol) in anhydrous CH_3CN (5 mL) was added and the mixture stirred at 60°C for 24 hours. The reaction mixture was then cooled to room temperature and filtered. The solids were washed twice with CH_3CN (20 mL), the combined organic layers were concentrated under reduced pressure and the crude material was purified by column chromatography (silica gel: 0–10% MeOH/CH_2Cl_2) to give the desired ligand **C14** (200 mg, 36%) as a brown oil. ^{1}H NMR (500 MHz, CD_3OD) δ: 8.16 (br m, 1H), 7.74 (br m, 1H), 7.63–7.02 (m, 16H), 5.12–4.85 (m, 3H), 4.02–1.95 (m, 24H), 1.5–1.3 (m, 9H), N-H signals not observed. ^{13}C NMR (125 MHz, CD_3OD) δ: 170.4, 170.2, 142.0, 141.4, 128.8, 128.7, 128.6, 128.5, 127.2, 127.1, 127.0, 126.5, 126.4, 126.3, 126.2, 57.5, 57.3, 56.9, 54.0, 50.7, 50.6, 49.9, 49.7, 49.5, 22.5, 22.4. HRMS (ESI+): calculated for $[M+H]^+$, $[C_{44}H_{58}N_9O_6]^+$ *m/z* 808.4432, found 808.4501.

Ln.C14

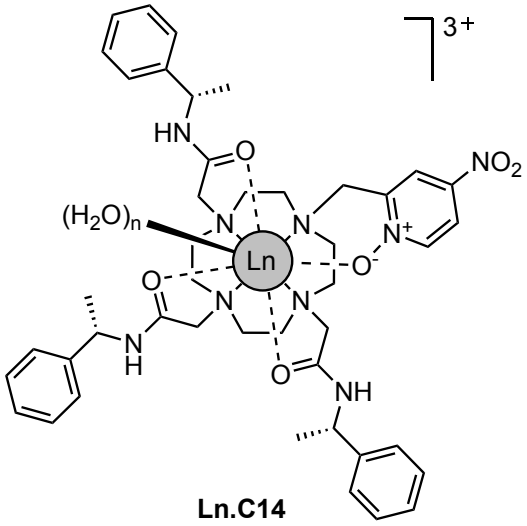

Ln.C14

To a solution of ligand **C14** (100 mg, 0.123 mmol) in a mixture of MeCN/H_2O (1:1, 6 mL) was added $LnCl_3.6H_2O$ (1.05 equiv., where Ln = Tb, Tm, Gd, Y) and the reaction mixture was stirred at 70 °C for 2 hours. Quantitative complexation was observed by LCMS analysis after this time. The organic solvent was removed under reduced pressure and the water was removed by freeze drying. The Ln complexes were obtained as white solids (120 mg, quant.) in each case. To remove residual salts, the complexes were subjected to reverse-phase HPLC [XBridge C18 column, gradient: 0 − 50% MeOH in 0.05% v/v formic acid, over 10 minutes at 17 mL per minute] to give **Tb.C14** (23 mg, 18%), **Tm.C14** (20.5 mg, 16%), **Gd.C14** (26 mg, 20%) and **Y.C14** (25 mg, 23%) as white solids. Analytical RP-HPLC analysis of each complex [XBridge C18 column, 0% MeOH for 5 minutes followed by 0 − 50% MeOH in 1% v/v formic acid over 10 minutes, at 0.7 mL per minute] revealed a single peak. HPLC retention times (RT) and mass spectral data for each [**Ln.C14**]$^{3+}$ complex is provided in the table below.

Complex	RT / min	Formula	Calculated m/z	Observed m/z
Tb.C14	16.12	$[C_{44}H_{54}N_9O_6Tb]^{3+}$	322.1223	322.1221
Tm.C14	16.24	$[C_{44}H_{55}N_9O_6Tm]^{3+}$	325.4586	325.4584
Gd.C14	16.13	$[C_{44}H_{55}N_9O_6Gd]^{3+}$	321.7885	321.7885
Y.C14	16.31	$[C_{44}H_{55}N_9O_6Y]^{3+}$	298.7825	298.7824

Extinction coefficients and quantum yields

Extinction coefficients of **Ln.C14** or **Ln.C14**-Cys (Ln = Tb or Eu) (1 mg/mL) were determined in 10 mM HEPES at pH 7.0. Quantum yields were measured using quinine sulfate in 0.05 M H_2SO_4 as a standard (Φ_{em}= 0.52, λ_{ex} = 350 nm).[2] The total emission intensity (450 – 720 nm) was determined for each complex and compared with quinine sulfate.

Luminescence experiments

Luminescence spectra were recorded on a Camlin Photonics luminescence spectrometer with FluoroSENS version 3.4.7.2024 software. Emission spectra were obtained using a 40 µL Hellma Analytics quartz cuvette (Art no. 111-10-K-40). Excitation light was set at 300 nm (or 300 nm for untagged Ln(III) complexes), and emission read in the range 400 – 720 using an integration time of 0.5 seconds, increment of 1.0 nm and excitation slit of 0.2 nm and emission slits of 0.5 nm.

Emission lifetime measurements were performed on the same instrument. Measurements were taken of 1 mL of 0.1 absorbance samples of **Tb.C14** in water. Measurements were obtained by indirect excitation of the Tb(III) ion *via* the pyridine antennae using a short pulse of light at λ_{max} (291 nm for untagged complex, 302 nm for cysteine-tagged complexes), followed by monitoring the integrated intensity of the light emitted at 545 nm, with 500 data points collected over a 10 millisecond time period. The decay curves were plotted in Origin Labs 2019 version 9.6.0.172, and fitted to the equation:

$$I = A_0 + A_1\, e^{-kt} \qquad (1)$$

where I is the intensity at time, t, following excitation, A_0 is the intensity when decay has ceased, A_1 is the pre-exponential factor and k is the rate constant for the depopulation of the excited state.

The hydration state, q, of **Tb.C14** and **Tb.C14**-Cys was determined using the modified Horrocks equation:

$$q(\mathrm{Tb}) = 5\,(1/\tau_{H2O} - 1/\tau_{D2O} - 0.06) \qquad (1)$$

where τ_{H2O} and τ_{D2O} are the emission lifetime times in water and D_2O, respectively, and *n* is the number of carbonyl-bound amide NH groups.[3]

Cysteine tagging reactions

Tb.C14 stocks were made up at 1 mg/mL in water and the pH adjusted to 8.0. Cysteine stocks were generally made to 10 or 100 mM in water and the pH adjusted to 8.0. **Tb.C14** (250 μM) and cysteine (2 mM) in 50 mM ammonium bicarbonate buffer, pH 8.0, were incubated at 37 °C for 24 hours. The reaction mixture was analysed by LCMS, UV-Vis and luminescence spectroscopy (following dilution, using λ_{exc} = 302 nm, λ_{em} = 400 – 720 nm).

Protein sample preparation

Uniformly ^{15}N-labelled ubiquitin S57C was produced in fusion with a C-terminal SerHis$_6$ tag as described previously.[4] The construct of ERp29 S114C contained a C-terminal His$_6$ tag, and the natural cysteine residue (Cys157) was mutated to serine. It was produced as described previously.[1]

Protein tagging reactions[§]

The tagging reaction of ubiquitin S57C was conducted at 4 °C with 0.1 mM protein in a buffer containing 20 mM HEPES, pH 7, and 4 mM dithiothreitol (DTT). After incubating at room temperature for 1 hour, excess DTT was washed out and the buffer was exchanged into a low-oxygen buffer (20 mM HEPES, pH 7, degassed by bubbling nitrogen gas through the solution for 4 hour) using an Amicon centrifugal filter tube with a molecular weight cutoff of 3 kDa. The ultrafiltration was conducted over 5 × 15 minutes in ambient atmosphere, using DTT-free buffer to wash out the DTT. The reduced protein was added slowly to a solution of the same volume and buffer containing 10 equivalents of the **Ln.C14** tag. The tagging reaction was performed in a glove box. After leaving the reaction mixture at room temperature overnight with shaking, the buffer was exchanged to NMR buffer (20 mM phosphate, pH 6.5).

The tagging reaction of ERp29 S114C with **Gd.C14** used the same protocol, except that degassed 20 mM HEPES, pH 7.5, was used as the buffer, and buffer exchanges used Amicon centrifugal filter tubes with a molecular weight cutoff of 10 kDa. The tagged

protein was exchanged into EPR buffer (20 mM MES in D_2O, pH 4.9; uncorrected pH meter reading), and 20% (v/v) perdeuterated glycerol were added.

Mass spectrometry

Intact protein analysis was performed on an Orbitrap Fusion™ Tribrid™ mass spectrometer (Thermo Fisher Scientific, USA) connected to a Thermo Fisher Scientific UltiMate 3000 HPLC system equipped with ZORBAX 300SB-C3, 3.5 μm, 4.6 x 50 mm HPLC column (Agilent Technologies, USA). Approximately 50 pmol of sample was injected using a 0.5 mL/min linear gradient of solvent A (0.1% (v/v) formic acid in water) and solvent B (0.1% (v/v) formic acid in acetonitrile), ramping solvent B from 5% solvent B at the start to 80% after 12 min. Data were collected using electrospray ionization in positive ion mode. Masses were determined by deconvolution using the program Xcalibur 3.0.63 (Thermo Fisher Scientific, USA).

Table S1. Photophysical data for the Tb(III) complexes of **C12** and **C14** and their cysteine derivatives (10 mM HEPES, pH 7.0, unless stated otherwise)

Complex	λ_{max}/nm	ε/$M^{-1}cm^1$	Φ_{em} /%	τ_{H2O} / ms	τ_{D2O}/ms	*q*
Tb.C12	300	1200	0.23	1.47	2.50	1.1
Tb.C12-Cys	278	15,500	20	1.48	2.40	1.0
Tb.C14	292	1800	0.1	0.557	0.835	2
Tb.C14-Cys	302	4600	0.4	0.282	0.539	1.6

[a] Values of hydration state *q* (±20%) were derived using literature methods.[3] Quantum yields were measured using quinine sulfate in 0.05 M H_2SO_4 as a standard (Φ_{em}= 52%).[2] Errors in quantum yields and lifetimes are ±15%.

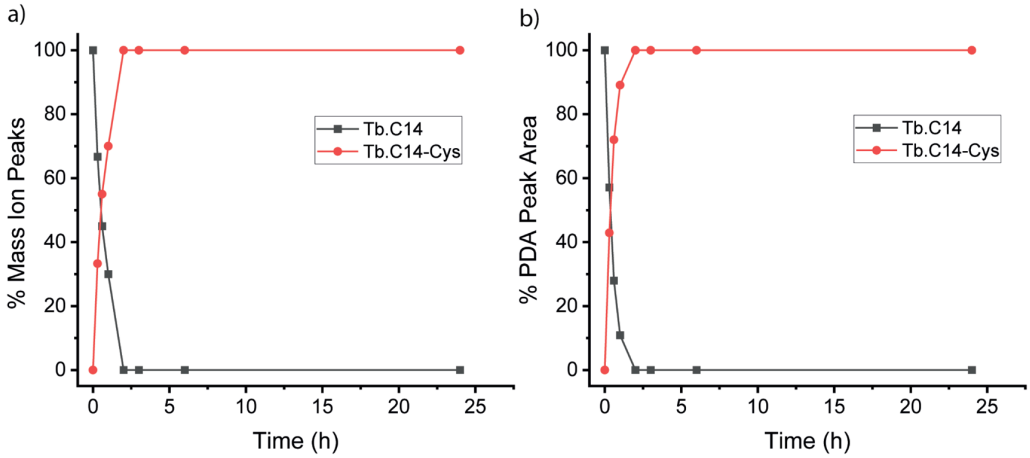

Figure S1. Monitoring the reaction between **Tb.C14** and cysteine by LCMS analysis. (a) percentage mass ion peaks of **Tb.C14** and **Tb.C14**-Cys, taken from total ion chromatogram, and plotted as a function of time; (b) Percentage PDA peak area of **Tb.C14** and **Tb.C14**-Cys plotted as a function of time, following incubation with cysteine (4 equivalents) in water at pH 8.0 and 37°C. Part (a) is reproduced from the main manuscript.

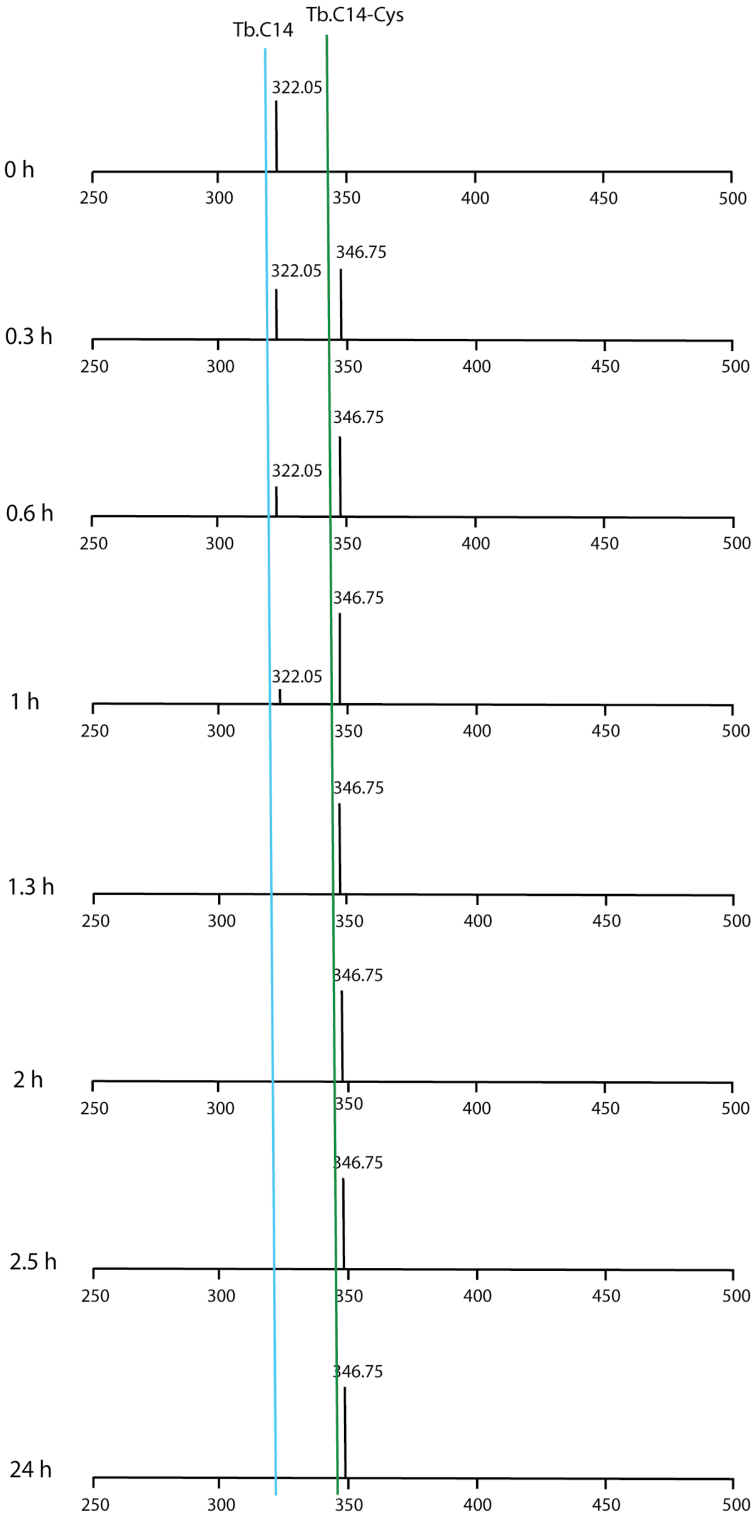

Figure S2. Mass spectra (ESI, positive mode) after incubation of **Tb.C14** (250 μM) with 4 equivalents of cysteine at 37 °C for 24 hours. Percentage conversion was calculated by comparing the intensity of the cysteine-tagged MS peak ([**Tb.C14**-Cys]$^{3+}$ m/z = 346.8) relative to the untagged peak ([**Tb.C14**]$^{3+}$ = 322.1).

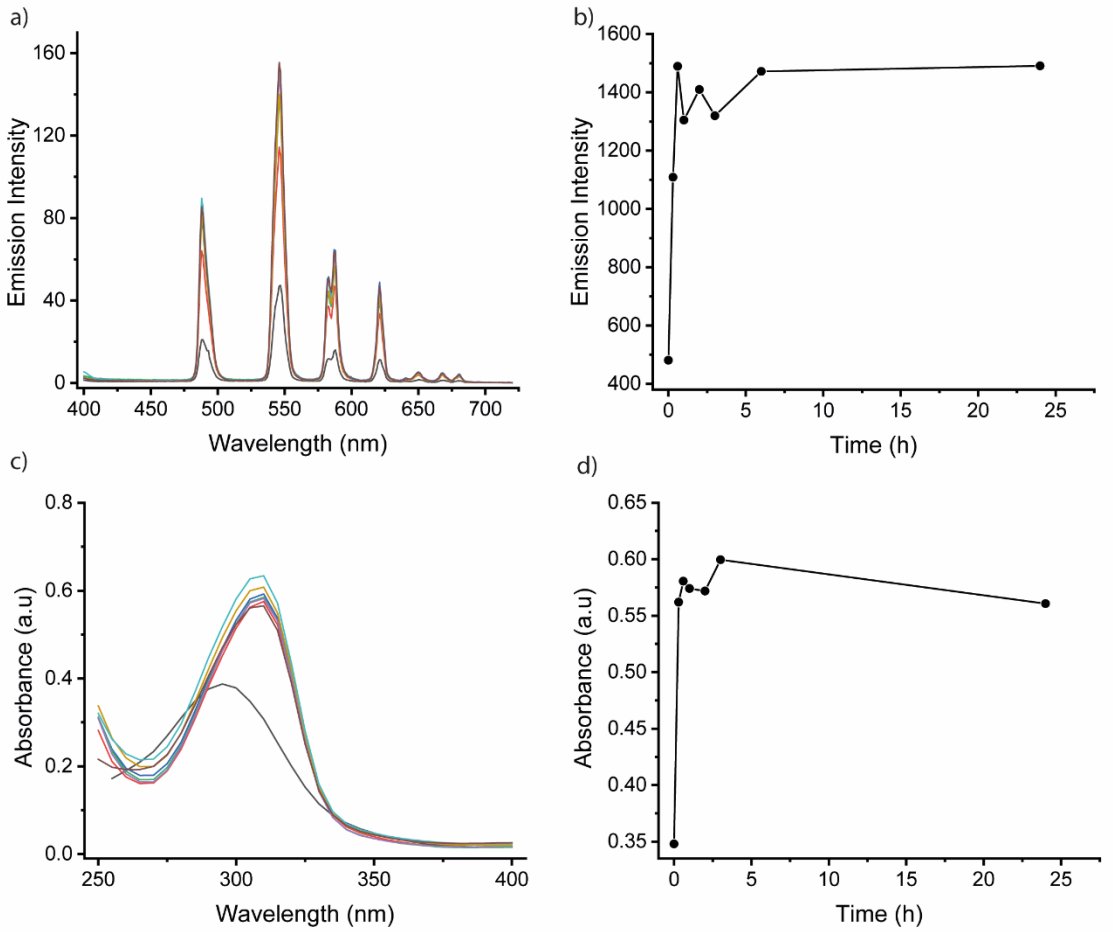

Figure S3. Monitoring the reaction between **Tb.C14** and cysteine using emission and UV-Vis spectroscopy. (a) Change in Tb(III) emission spectra; and (b) emission intensity between 535–565 nm of **Tb.C14** as a function of time. (c) Change in absorption spectra; and (d) absorbance at 300 nm of **Tb.C14** (250 μM) as a function of time, following incubation with cysteine in 50 mM ammonium bicarbonate buffer at pH 8.0 and 37°C.

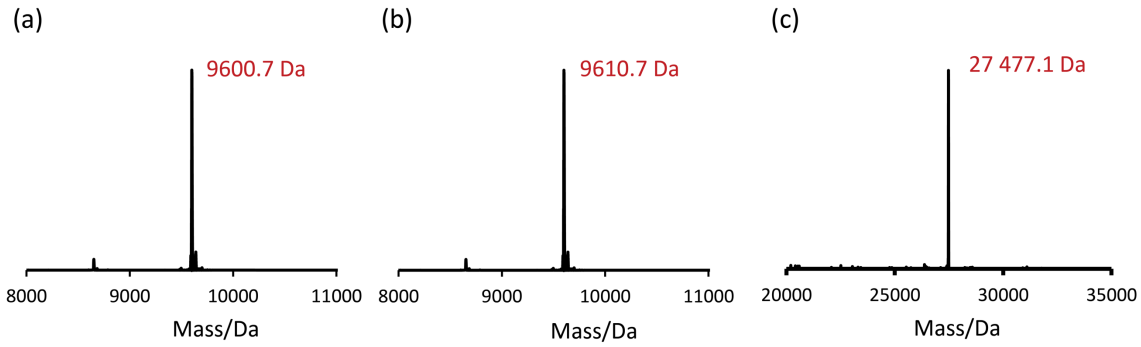

Figure S4. Mass spectra of proteins tagged with **Tm.C14** and **Gd.C14** tags. (a) Ubiquitin S57C tagged with **Tb.C14** (expected mass: 9604.2 Da). (b) Ubiquitin S57C tagged with **Tm.C14** (expected mass: 9614.2 Da). (c) ERp29 tagged with **Gd.C14** (expected mass: 27,480.1 Da).

NMR spectroscopy

All NMR spectra were recorded at 25 °C. 2D NMR spectra were measured on a Bruker 800 MHz NMR spectrometer equipped with a TCI cryoprobe.

Table S2. Δχ tensors fitted to ubiquitin S57C with **C12** and **C14** tags, showing the complete set of parameters fitted.[a]

Tag	$\Delta\chi_{ax}$ /10^{-23} m^3	$\Delta\chi_{rh}$ /10^{-23} m^3	*x*/Å	*y*/Å	*z*/Å	α	β	γ	*Q*
Tm.C14	8.9	0.5	19.786	14.408	14.266	165°	90°	109°	0.05
Tb.C14	-10.9	-1.6	19.786	14.408	14.266	164°	86°	117°	0.04
Tm.C12	5.8	3.0	24.296	14.337	14.788	32°	124°	11°	0.06
Tb.C12	8.3	3.3	24.296	14.337	14.788	60°	56°	87°	0.01

[a] Same as Table 1 in the main text, except that the coordinates of the fitted metal ion are provided too, along with the Euler angles of the Δχ tensors relative to the structure 1UBQ.[5]

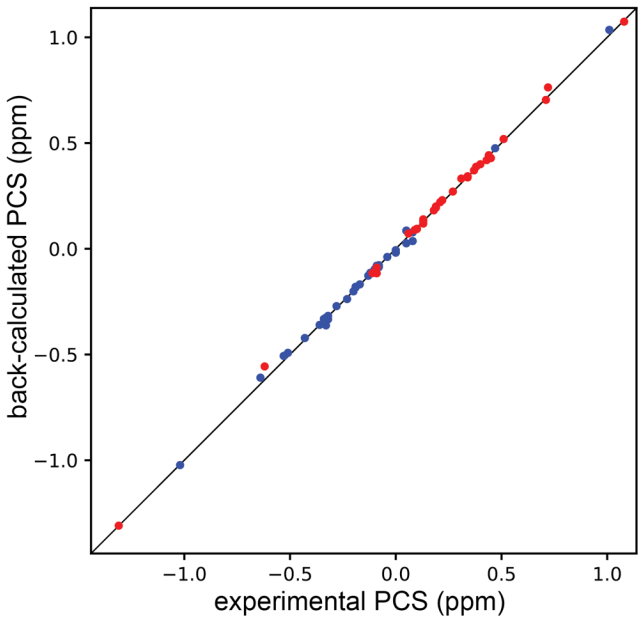

Figure S5. Correlation between back-calculated and experimental backbone amide proton PCSs. Red and blue points identify PCSs measured with **Tb.C14** and **Tm.C14** tags, respectively.

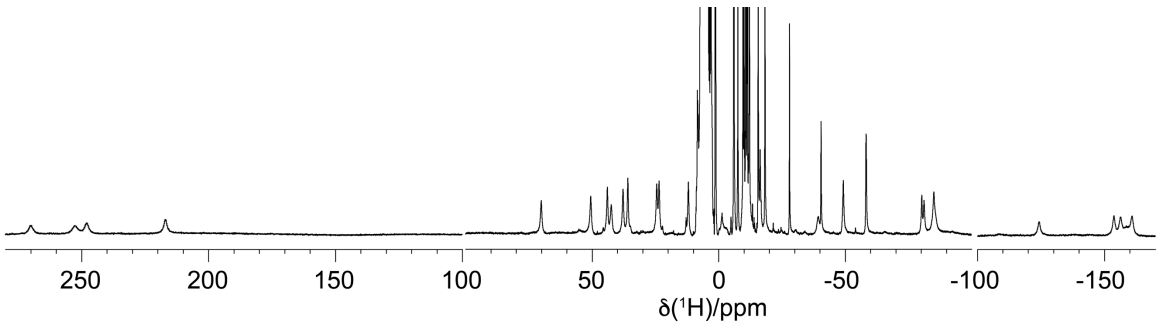

Figure S6. 1D ^{1}H-NMR spectrum of the **Tm.C14** tag. The spectrum was recorded of a 14 mM solution in 20 mM HEPES buffer, pH 7, at 25 ^{o}C using a Bruker 400 MHz NMR spectrometer equipped with a room temperature probe. The spectrum shown was recorded in three segments, with the carrier frequencies set at the water frequency (4.7 ppm), 200 ppm and -100 ppm, respectively, to avoid poor excitation due to off-resonance effects.

Table S3. Pseudocontact shifts measured in ppm for backbone amide protons of ubiquitin S57C ligated with **Tb.C14** or **Tm.C14**.

Residue	PCS with Tb^{3+}	PCS with Tm^{3+}
Gln 2	0.31	-0.33
Ile 3	0.27	-0.28
Phe 4	0.34	-0.32
Val 5	0.19	-0.19
Lys 6	0.22	-0.20
Thr 7	0.13	-0.12
Leu 8	0.13	-0.10
Gly 10	0.10	-0.09
Lys 11	0.09	-0.08
Thr 12	0.10	-0.08
Ile 13	0.13	-0.13
Leu 15	0.18	-0.19
Val 17	0.19	-0.23
Thr 22	-1.31	1.01
Leu 25	-0.62	0.47
Val 27	-0.09	0.05
Lys 29	-0.09	0.05
Asp 32	-0.15	0.08
Glu 34	0.00	0.00
Gly 35	-0.02	0.00
Ile 36	0.00	0.00
Asp 39	-0.06	0.05
Gln 41	0.06	-0.04
Leu 43	0.34	
Ile 44	0.43	-0.34
Phe 45	0.72	-0.64
Gly 47	0.45	-0.33
Leu 50	0.71	-0.53
Asp 58	-0.11	0.08
Gln 62	1.08	-1.02
Glu 64	0.44	-0.43
Ser 65	0.51	-0.51
Thr 66	0.38	-0.36
Leu 67	0.37	-0.33
His 68	0.40	-0.32
Val 70	0.21	-0.17

EPR spectroscopy

All EPR measurements were performed at 10 K on a modified Bruker EPR spectrometer operating at W-band (94 GHz).[6]

EPR lineshape measurement

The line shape of the protein-bound **Gd.C14** was measured by an electron spin-echo (ESE) field-sweep sequence $\pi/2 - \tau - \pi -$ echo, using $\pi/2 = 40$ ns, $\pi = 80$ ns and $\tau = 400$ ns. T_1 relaxation was measured by the inversion recovery sequency $\pi - (t + \mathrm{d}t) - \pi/2 - \tau - \pi -$ echo. The integrated echo intensity was recorded as a function of time t incremented in intervals $\mathrm{d}t$ (1000 ns), using the same pulse lengths as above. T_2 (phase memory) relaxation was measured by recording the decay of the integrated echo intensity with time, using the pulse sequence $\pi/2 - (t + \mathrm{d}t) - \pi - (t + 2\mathrm{d}t) -$ echo ($\mathrm{d}t = 20$ ns). The relaxation data (Fig. S4) was fit using a MATLAB least squares fitting algorithm to the stretched exponential functions as detailed in Table S2.

DEER measurements

The standard four-pulse DEER sequence ($\pi/2(\nu_{\mathrm{obs}}) - t_1 - \pi(\nu_{\mathrm{obs}}) - (t_1 + \mathrm{d}t) - \pi(\Delta\nu_{\mathrm{pump}}) - (t_2 - \mathrm{d}t) - \pi(\nu_{\mathrm{obs}}) - t_2 -$ echo) was used with τ-averaging, where the time domain spectrum is acquired by averaging traces with different t_1 (τ) values. Specifically, each scan was acquired by averaging four different τ values from 400 – 562 ns. The DEER echo was observed at 93.960 GHz with $\pi/2$ and π pulses of 16 ns and 32 ns, respectively, and an ELDOR (pump) pulse of $\pi = 16$ ns at 94.035 GHz. The field position for detection was set at the peak of the Gd^{3+} spectrum (Fig. S5) such that the pump pulse was applied at approximately the centre of the Gd spectrum, and the probe pulse was applied on the edge, with 75 MHz separation between the two. These frequency positions were checked by microwave nutation – i.e. shifting the microwave frequency until the nutation measurement gave a 64 ns period ($\pi = 32$ ns) at the probe frequency, and a period of 32 ns ($\pi = 16$ ns) at the pump frequency. Other parameters used were a repetition time of 255 μs, increment $\mathrm{d}t = 20$ ns, 10 shots per point and $t_2 = 7.2$ μs.

The data were analysed using DeerAnalysis2019[7] and distance distributions were obtained using Tikhonov regularization. The regularization parameter was obtained using

the L-curve criterion. Estimates of the uncertainties in distance distributions due to background correction were obtained using the validation option in DeerAnalysis.

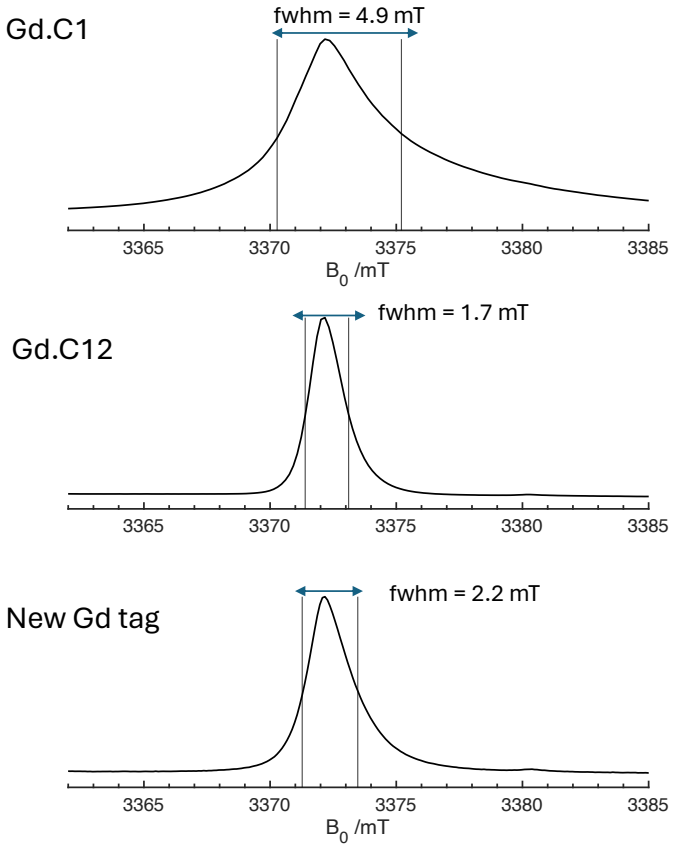

Figure S7. Comparison of the EPR lineshapes of the **Gd.C1**[4], **Gd.C12** and new **Gd.C14** tags, annotated with the linewidth (fwhm) of the central –½ to ½ transition.

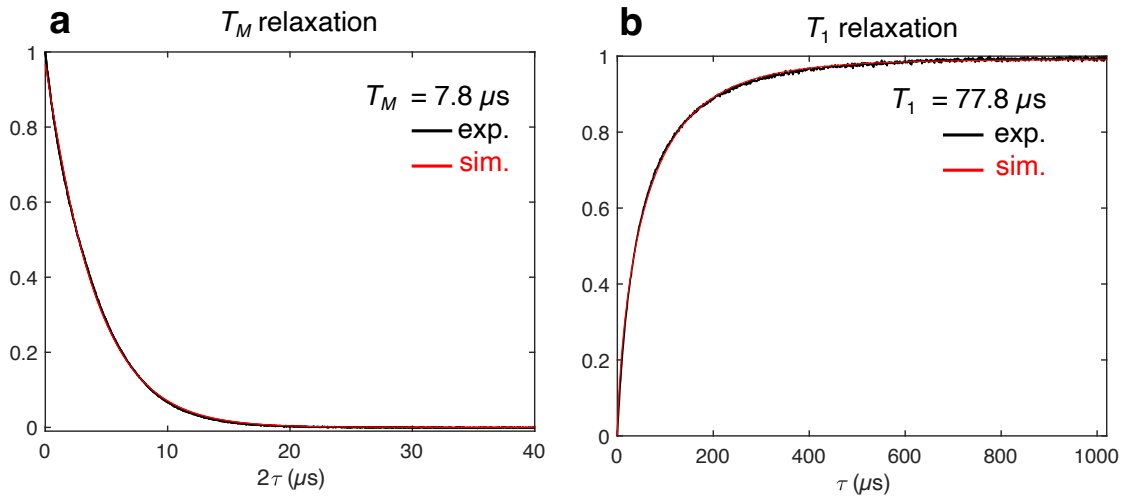

Figure S8. Relaxation curves (black traces) and fits (red traces). (a) T_1 relaxation data and fits using the stretched exponential fitting function described in Table S3. The mean best fit T_1 value is annotated beside each curve. (b) T_M relaxation data and fits using the stretched exponential fitting function described in Table S3. The mean best fit T_M value is annotated beside each curve.

Table S4. T_1 and T_M relaxation times determined for the **Gd.C14** and **Gd.C12** tags.[a]

Sample	$\overline{T_1}$ (τ_1, α) / μs	$\overline{T_M}$ (τ_2, α) / μs
Gd.C14	77.8 (63.1, 0.72)	7.8 (8.1, 1.06)
Gd.C12	90.5 (77.1, 0.76)	8.4 (8.9, 1.1)

[a] T_1 relaxation data were fitted by the stretched exponential function $f_{T1} = A\left(1 - \exp\left[-\left(\frac{x}{\tau_1}\right)^{\alpha}\right]\right)$. The average T_1 time was calculated using the gamma function distribution $\overline{T_1} = \frac{\tau_1}{\alpha} \cdot \mathbf{\Gamma}\left(\frac{1}{\alpha}\right)$. T_2 relaxation data were fitted by the stretched decay exponential function $f_{TM} = A \exp\left[-\left(\frac{2x}{\tau_2}\right)^{\alpha}\right]$. The average T_2 time of each stretched exponential fit was calculated assuming the gamma function distribution $\overline{T_2} = \frac{\tau_2}{\alpha} \cdot \mathbf{\Gamma}\left(\frac{1}{\alpha}\right)$.

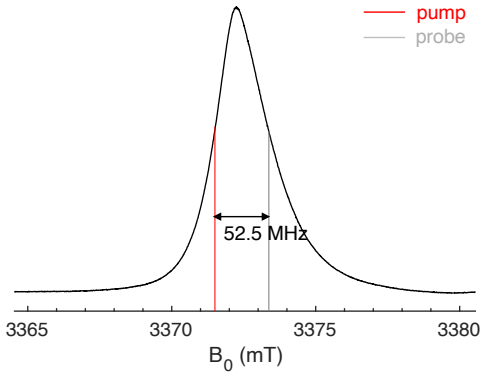

Figure S9. Central –½ to ½ transition of the EPR spectrum of the **Gd.C14** tag following attachment to ERp29 S114C. The spectrum is annotated with the DEER pump and probe pulse positions, which are separated by 75 MHz (1.8 mT). The sample concentration was 80 μM.

Notes and References

[§] The tagging conditions differed between the reactions with free cysteine and protein. When tagging free cysteine, the cysteine was in four-fold excess over the tag. The pH was 8 and the temperature 37 ºC. When tagging the proteins, the tag was in ten-fold excess over the protein. The pH was 7 and the temperature room temperature. The tagging reaction of the proteins is thus expected to be slower. We chose the lower pH to increase the stability of the cysteine thiol group towards oxidation. This was important when the reducing agent (DTT) was removed by repeated ultrafiltration with buffer. In our experiments with the proteins, we did the tagging reaction overnight. We conclude from the competitive formation of proteins dimerized via a disulfide bond that the oxidation reaction competed with the tagging reaction. Therefore, the removal of DTT should preferably be performed in an inert atmosphere to minimize unwanted oxidation.

1. I. D. Herath, C. Breen, S. H. Hewitt, T. R. Berki, A. F. Kassir, C. Dodson, M. Judd, S. Jabar, N. Cox, G. Otting and S. J. Butler, *Chem. Eur. J.*, 2021, **27**, 13009-13023.

2. K. Suzuki, A. Kobayashi, S. Kaneko, K. Takehira, T. Yoshihara, H. Ishida, Y. Shiina, S. Oishi and S. Tobita, *Phys.Chem. Chem. Phys.*, 2009, **11**, 9850-9860.

3. A. Beeby, I. M. Clarkson, R. S. Dickins, S. Faulkner, D. Parker, L. Royle, A. S. de Sousa, J. A. Gareth Williams and M. Woods, *J. Chem. Soc., Perkin Trans. 2*, 1999, **0**, 493-504.

4. H. W. Orton, E. H. Abdelkader, L. Topping, S. J. Butler and G. Otting, *Magn. Reson.*, 2022, **3**, 65-76.

5. S. Vijay-Kumar, C. E. Bugg and W. J. Cook, *J. Mol. Biol.*, 1987, **194**, 531-544.

6. A. Nalepa, K. Möbius, W. Lubitz and A. Savitsky, *J. Magn. Reson.*, 2014, **242**, 203-213.

7. G. Jeschke, V. Chechik, P. Ionita, A. Godt, H. Zimmermann, J. Banham, C. R. Timmel, D. Hilger and H. Jung, *Appl. Magn. Reson.*, 2006, **30**, 473-498.